The *XMM* Cluster Survey: predicted overlap with the *Planck* Cluster Catalogue

Pedro T. P. Viana,[1,2] António da Silva,[1] Elsa P. R. G. Ramos,[1,2] Andrew R. Liddle,[3]
E. J. Lloyd-Davies,[3] A. Kathy Romer,[3] Scott T. Kay,[4] Chris A. Collins,[5] Matt Hilton,[6]
Mark Hosmer,[3] Ben Hoyle,[7,8,9] Julian A. Mayers,[3] Nicola Mehrtens,[3]
Christopher J. Miller,[10] Martin Sahlén,[11] S. Adam Stanford[12,13] and John P. Stott[5,14]

[1]*Centro de Astrofísica, Universidade do Porto, Rua das Estrelas, 4150-762 Porto, Portugal*
[2]*Departamento de Física e Astronomia, Faculdade de Ciências, Universidade do Porto, Rua do Campo Alegre, 687, 4169-007 Porto, Portugal*
[3]*Astronomy Centre, University of Sussex, Falmer, Brighton BN1 9QH*
[4]*Jodrell Bank Centre for Astrophysics, School of Physics and Astronomy, The University of Manchester, Manchester M13 9PL*
[5]*Astrophysics Research Institute, Liverpool John Moores University, Twelve Quays House, Egerton Wharf, Birkenhead CH41 1LD*
[6] *School of Physics & Astronomy, University of Nottingham, Nottingham NG7 2RD*
[7]*Institut de Ciéncies del Cosmos (ICCUB-IEEC), Departamento de Física, Martí i Franqués 1, 08034 Barcelona, Spain*
[8]*Institute of Cosmology and Gravitation, Dennis Sciama Building, Burnaby Road, Portsmouth PO1 3FX*
[9]*Helsinki Institute of Physics, P.O. Box 64, University of Helsinki, FIN-00014 Helsinki, Finland*
[10]*Astronomy Department, University of Michigan, Ann Arbor, MI 48109, USA*
[11]*The Oskar Klein Centre for Cosmoparticle Physics, Department of Physics, Stockholm University, SE-106 91 Stockholm, Sweden*
[12]*Physics Department, University of California, Davis, CA 95616, USA*
[13]*Institute of Geophysics and Planetary Physics, Lawrence Livermore National Laboratory, Livermore, CA 94551, USA*
[14]*Department of Physics, Institute for Computational Cosmology, Durham University, South Road, Durham DH1 3LE*

ABSTRACT

We present a list of 15 clusters of galaxies, serendipitously detected by the *XMM* Cluster Survey (XCS), that have a high probability of detection by the *Planck* satellite. Three of them already appear in the *Planck* Early Sunyaev–Zel'dovich (ESZ) catalogue. The estimation of the *Planck* detection probability assumes the flat Lambda cold dark matter (ΛCDM) cosmology most compatible with 7-year *Wilkinson Microwave Anisotropy Probe* (*WMAP*7) data. It takes into account the XCS selection function and *Planck* sensitivity, as well as the covariance of the cluster X-ray luminosity, temperature and integrated Comptonization parameter, as a function of cluster mass and redshift, determined by the Millennium gas simulations. We also characterize the properties of the galaxy clusters in the final data release of the XCS that we expect *Planck* will have detected by the end of its extended mission. Finally, we briefly discuss possible joint applications of the XCS and *Planck* data.

Key words: galaxies: clusters: general.

1 INTRODUCTION

The properties of the intergalactic medium within clusters of galaxies can be studied using observational data obtained both in the X-ray and sub-millimetre/millimetre (sub-mm/mm) wavebands. These methods are complementary and can be combined not only to better characterize the internal structure of galaxy clusters, but also to derive the angular-diameter distance as a function of redshift thus helping to constrain cosmological parameters (see Carlstrom, Holder & Reese 2002, for a review).

The study of galaxy clusters in X-rays, through the bremsstrahlung emission and line emission of the intracluster medium (ICM), started significantly earlier than in the sub-mm and mm wavelengths through the Sunyaev–Zel'dovich (SZ) effect they produce. Large catalogues of galaxy clusters assembled through their identification in X-rays have been created since the *ROSAT* data became available (Ebeling et al. 1998; Rosati et al. 1998; De Grandi et al. 1999; Böhringer et al. 2000; Romer et al. 2000; Henry et al. 2001; Cruddace et al. 2002; Perlman et al. 2002; Mullis et al. 2003; Böhringer et al. 2004; Burenin et al. 2007) more than a decade ago, while similar catalogues assembled through identification of galaxy clusters via the SZ effect are only now being generated (Marriage et al. 2010; Vanderlinde et al. 2010; Williamson et al.

⋆E-mail: viana@astro.up.pt

2011). Among the X-ray and SZ cluster surveys under way, the *XMM* Cluster Survey (XCS, Lloyd-Davies et al. 2011; Mehrtens et al. 2011) and the *Planck* Cluster Survey (Planck Collaboration 2011a) stand out for the very large number of galaxy clusters they are expected to detect. Both surveys are based on the identification of galaxy clusters in satellite data, from *XMM–Newton*[1] (*XMM* hereafter) and the *Planck* satellite (*Planck*), respectively.

Although the SZ effect can be used on its own to constrain the properties of the ICM, the usefulness of the information it contains is maximized when X-ray data is also available (Carlstrom et al. 2002). This is particularly true in the case of the galaxy clusters expected to be detected by *Planck*, because of the limited information content of the expected SZ-related data, due to the low angular resolution and sensitivity (for galaxy cluster studies) of *Planck*. Ideally, the galaxy clusters for which *Planck* will be able to best characterize their SZ signal would be re-observed with *XMM* or *Chandra*. However, it is not clear that this can be done on a large scale. It is therefore important to consider alternative sources of X-ray data for (at least some of) the clusters in the *Planck* Cluster Survey.

The aim of this paper is to identify and present the clusters of galaxies in the XCS first data release, for which X-ray temperatures have been estimated, that have the highest probability of also being detected by *Planck*. We will also characterize the distribution of the properties of the galaxy clusters that we expect will be detected both by XCS and *Planck*, and discuss possible applications of the information contained in the data gathered by both surveys on those galaxy clusters.

The structure of this paper is as follows. We start by reviewing the characteristics of the XCS and the *Planck* Cluster Survey. Next, we present the methodology we used to estimate the probability of detection of an XCS galaxy cluster by *Planck*, and characterize the expected overlap between the two surveys. We then discuss possible applications of the data gathered by both XCS and *Planck* on the galaxy clusters present in the joint sample.

2 THE *XMM* AND *Planck* CLUSTER SURVEYS

2.1 *XMM* Cluster Survey

The XCS collaboration is carrying out a systematic search for serendipitous detections of clusters of galaxies in the outskirts of publicly available pointings in the *XMM* archive (Romer et al. 2001). A fully automated procedure is in place, which allows the identification and classification of all sources in such pointings (Lloyd-Davies et al. 2011). XCS cluster candidates are those sources that are classified as being more extended than the instrument point spread function. The available X-ray and optical data, including information from the literature, is then used to determine if such candidates can be confirmed as genuine galaxy clusters and to estimate their redshifts (Mehrtens et al. 2011). Finally, an X-ray spectroscopy analysis is carried out, using the archival *XMM* data, and the ICM temperature estimated if enough X-ray photon counts are available.

The XCS project is ongoing, but already 5776 *XMM* pointings have been analysed, yielding a serendipitous cluster candidate catalogue numbering 3675 entries (Lloyd-Davies et al. 2011). Among these, we were able to optically confirm the presence of 503 clusters of galaxies, of which 255 are new to the literature and 356 are new X-ray discoveries, while 464 have a redshift estimate and 402 had their X-ray temperatures measured (Mehrtens et al. 2011).

So far, the XCS covers a combined area close to 410 deg^2 suitable for cluster searching, taking into account overlapping and repeated exposures, and excluding regions of low Galactic latitude, the Magellanic Clouds and pointings with very extended central targets (Lloyd-Davies et al. 2011). Given that the XCS has only analysed the *XMM* observations performed up to mid-2009, and the mission lifetime has been extended until the end of 2014, a conservative estimate for the final XCS area for cluster searching is about 600 deg^2.

The XCS will be the largest catalogue of X-ray selected clusters ever compiled. It is expected to contain several thousand entries, more than 20 per cent of which will have an associated X-ray temperature derived from the serendipitous data alone (Sahlén et al. 2009). The XCS will be accompanied by a complete description of its selection function, making it a valuable resource for the unbiased derivation of cluster scaling relations and cosmological parameters. The XCS selection function is derived by placing a sample of mock surface-brightness profiles into real *XMM* observation data files. These profiles were produced assuming a simple symmetrical model for the ICM structure (for more details see Sahlén et al. 2009). This assumption has been validated by an investigation of the recovery rate of clusters with profiles drawn from the CLEF hydrodynamical simulation (Kay et al. 2007), including clusters with cool cores and substructure, which has shown no significant change in the XCS detection efficiency (Lloyd-Davies et al. 2011).

2.2 *Planck* Cluster Survey

The *Planck* satellite has nine frequency channels ranging from 30 to 857 GHz, with an angular resolution reaching 5 arcmin for the frequency channels above 143 GHz. Its objective is to characterize the temperature anisotropies and polarization of the cosmic microwave background radiation. These include anisotropies produced via the SZ effect in the direction of galaxy clusters. Their characteristic frequency dependence and expected profiles can be used to extract cluster candidates and their integrated Comptonization parameter. Most recent analyses suggest that during its original nominal 14-month mission, *Planck* will be able to detect around 2000 galaxy clusters (Melin, Bartlett & Delabrouille 2006; Bartlett et al. 2008; Leach et al. 2008; Chamballu, Bartlett & Melin 2010).

The *Planck* Early Sunyaev–Zel'dovich (ESZ) catalogue has now been released, and contains 189 galaxy clusters detected with a signal-to-noise higher than six (Planck Collaboration 2011b), of which 20 were previously unknown. An extended mission for *Planck* is already underway, which is expected to roughly double the observing time with respect to the nominal *Planck* mission (Planck Collaboration 2011a).

3 METHODOLOGY

The probability of detection by *Planck* of an XCS galaxy cluster, with X-ray luminosity L and temperature T, is given by

$$P(>Y_{min}|L, T) = \frac{P(>Y_{min}, L, T)}{P(L, T)}, \qquad (1)$$

where we are assuming that all the clusters with an integrated Comptonization parameter, Y, above Y_{min}, and only these, are detected by *Planck*. This has been shown by Melin et al. (2006) to be a good approximation for the *Planck* sensitivity, as long as Y_{min} is allowed to vary as a function of the cluster angular size. We use the information in fig. 2 of Melin et al. (2006) to model this dependence, as a function of the angular size of the cluster core radius, θ_c, in the context

of an isothermal β-model with $\beta = 2/3$. Also from fig. 2 in Melin et al. (2006), it can be inferred that the *Planck* detection limit for unresolved clusters, in terms of Y defined within the virial radius, is around 1×10^{-3} arcmin^2 for a signal-to-noise ratio of 5 (nominal *Planck* mission), the minimum necessary for a reliable estimation of Y from *Planck* data (Melin et al. 2006). However, an analysis of the characteristics of the *Planck* ESZ catalogue suggests that it is more appropriate to consider 1×10^{-3} arcmin^2 as the *Planck* detection limit for unresolved clusters when Y is defined within a sphere encompassing a density contrast 200 times the critical density, i.e. within r_{200} (Planck Collaboration 2011b). Therefore, we assume

$$Y_{\min} = 9 \times 10^{-4} \exp(0.7\,\theta_{\rm c}^{0.8})\ \mathrm{arcmin}^2 \tag{2}$$

to be valid for $\theta_{\rm c} > 0.1$ in arcmin, with $Y_{\min}$ being the SZ integrated signal within r_{200} and consider the *Planck* detection limit for unresolved clusters to be reached for lower values of $\theta_{\rm c}$. This sensitivity also represents a reasonable extrapolation of the sensitivity achieved in the *Planck* ESZ survey (Planck Collaboration 2011b), when it is taken into account that the ESZ clusters that have signal-to-noise ratio above six were detected in just 10 months of *Planck* data, the Y values estimated by the *Planck* collaboration are within $5R_{500}$, and most of the ESZ clusters appear as extended in the *Planck* maps. With the extension of the *Planck* mission, the detection limit goes down proportionally by a factor of roughly $\sqrt{2}$, given that the extended mission has a duration that is approximately double that of the nominal mission. Thus, in the case of the extended mission, for each $\theta_{\rm c}$, the associated $Y_{\min}$ is calculated by dividing the result one obtains using equation (2) by $\sqrt{2}$. The XCS selection function was estimated assuming the cluster structure to be well approximated by an isothermal β model with $\beta = 2/3$, plus a universal core radius of 160 kpc (Sahlén et al. 2009). Therefore, in order to be consistent, we make the latter assumption when calculating $Y_{\min}$, which means this quantity will be the same for all clusters at a given redshift.

In order to determine $P(>Y_{\min}|L, T)$, we need to know both $P(>Y_{\min}, L, T)$ and $P(L, T)$ as a function of redshift. These quantities can be obtained by integrating the joint probability function $P(L, T, Y)$, as follows

$$P(> Y_{\min}, L, T) = \int_{Y_{\min}}^{\infty} P(L, T, Y)\mathrm{d}Y\,, \tag{3}$$

and

$$P(L, T) = \int_{0}^{\infty} P(L, T, Y)\mathrm{d}Y\,. \tag{4}$$

The full characterization of $P(L, T, Y|M)$, as a function of redshift, has been done only by Stanek et al. (2010), using the data generated by the Millennium gas simulations (MGS). Therefore, we use their results,[2] namely those derived from the MGS with pre-heating, to estimate $P(L, T, Y)$ through

$$P(L, T, Y) = \int_{M_{\min}}^{M_{\max}} P(L, T, Y|M)P(M)\mathrm{d}M\,, \tag{5}$$

where

$$P(M) = \frac{n(M)}{\int n(M)\mathrm{d}M}\,, \tag{6}$$

with the integration going from $M_{\min} = 5 \times 10^{13}\,h^{-1}\,\mathrm{M}_{\odot}$ to $M_{\max} = 5 \times 10^{15}\,h^{-1}\,\mathrm{M}_{\odot}$. The lower limit coincides with the MGS

---

[2] Note that the units of Y should be taken to be $h^{-1}\,\mathrm{Mpc}^2$ in the derived MGS scaling relations between this quantity and cluster mass (G. Evrard and R. Stanek, private communication).

mass cut-off and h is the value of the Hubble constant in units of $100\,\mathrm{km\,s^{-1}\,Mpc^{-1}}$. The halo mass M is defined as that which is contained within a sphere encompassing a density contrast 200 times the critical density, i.e. within r_{200}. All other cluster properties mentioned in this work, namely those that appear in Table 1 and Fig. 3, also refer to r_{200}. The mass function, $n(M)$, is derived following Jenkins et al. (2001) and Hu & Kravtsov (2003), for a spatially flat cold dark matter cosmology with a spectrum of primordial adiabatic Gaussian density perturbations and the presence of a cosmological constant, Λ. We assume $\Omega_{\rm c} = 0.23$, $\Omega_{\rm b} = 0.04$, $\Omega_{\Lambda} = 0.73$, $n_{\rm s} = 0.97$, $\sigma_8 = 0.81$ and $h = 0.70$, motivated by the 7-year *Wilkinson Microwave Anisotropy Probe* (*WMAP*7) results (Komatsu et al. 2010).

Both the X-ray luminosity and temperature of the XCS clusters are measured with some associated uncertainty. What we then need to know is the probability of an XCS cluster having some X-ray luminosity, L, and temperature, T, given the measured values, respectively $L_{\rm obs}$ and $T_{\rm obs}$, for those quantities, i.e. $P[(L, T)|(L_{\rm obs}, T_{\rm obs})]$. This probability is different for each XCS cluster, and its effect on the probability of detection by *Planck* of an XCS galaxy cluster, with measured $L_{\rm obs}$ and $T_{\rm obs}$, can be taken into account by marginalizing over L and T, as follows:

$$P_{\rm full}(>Y_{\min}|L_{\rm obs}, T_{\rm obs}) = \int_{0}^{\infty} \int_{0}^{\infty} P(>Y_{\min}|L, T) \\ \times P[(L, T)|(L_{\rm obs}, T_{\rm obs})]\mathrm{d}T\,\mathrm{d}L\,. \tag{7}$$

Naively, for each XCS galaxy cluster, the quantity $P[(L, T)|(L_{\rm obs}, T_{\rm obs})]$ would simply be taken to be the joint probability distribution of the estimated $L_{\rm obs}$ and $T_{\rm obs}$ values, based on the data collected for that cluster. This would be the case if we assumed we had no (prior) knowledge about the properties of the underlying galaxy cluster population and of the way we built the cluster sample under analysis, i.e. of the sample selection function. However, we not only already had to make assumptions about the underlying galaxy cluster population, in order to be able to estimate $P(> Y_{\min}|L, T)$, but we also believe we know how the XCS selection function, $f_{\rm XCS}(L, T)$, behaves. Therefore, we need to include these prior assumptions in the estimation of $P[(L, T)|(L_{\rm obs}, T_{\rm obs})]$. This can be done, for each XCS galaxy cluster, by multiplying the joint probability distribution of the estimated $L_{\rm obs}$ and $T_{\rm obs}$ values, based on the data collected for that cluster, by the probability of a cluster with L and T being present in the XCS catalogue, which is equal to the product of $f_{\rm XCS}(L, T)$ and $P(L, T)$, and by a renormalization constant that ensures the integral of $P[(L, T)|(L_{\rm obs}, T_{\rm obs})]$ over all possible L and T is unity.

In the following section, we will use the methodology just described to determine the probability of *Planck* detection for galaxy clusters in the XCS first data release, and to characterize the expected overlap between the XCS and *Planck* Cluster Survey. This methodology can, in principle, be applied to any two or more cluster surveys, for example *eROSITA* (Cappelluti et al. 2011), DES (Annis et al. 2005) or SPT (Carlstrom et al. 2011), in order to derive the expected number and properties of the objects common to those surveys being considered.

4 RESULTS AND DISCUSSION

We have calculated $P_{\rm full}(>Y_{\min}|L, T)$ only for those galaxy clusters in the XCS first data release which have a minimum of 250 X-ray photon counts, as otherwise the estimates of the X-ray observables would be too uncertain. Further, we have only considered clusters which have a X-ray temperature in excess of 2 keV and a redshift in the interval $0.1 < z < 1.0$ (the XCS selection function has not yet

Table 1. All clusters in the XCS250 sample and $P_{full}(>Y_{min}|L, T) > 0.5$ in the case of the *Planck* extended mission. The bolometric ([0.05, 100] keV band) luminosities, L_{bol}^d and L_{bol}, X-ray temperatures, T_X^d and T_X and integrated Comptonization parameter, Y, are defined within r_{200} and have units of 10^{44} erg s^{-1}, keV and $10^{-4} h^{-2}$ Mpc^2, respectively. The uncertainty in the estimation of these quantities has a probability distribution which is close to log-normal, and the interval of variation presented corresponds to the 68 per cent confidence interval. The quantities (L_{bol}^d, T_X^d) and (L_{bol}, T_X) differ in that the estimation of the latter takes into account the (prior) assumptions made in this work, with respect to the cosmological model, cluster scaling relations and XCS selection function. The probability of *Planck* detection, $P_{full}(>Y_{min}|L, T)$, is shown in the last column for both the nominal and extended missions (nominal/extended). The clusters with an asterisk next to their XCS name already appear in the *Planck* ESZ catalogue (Planck Collaboration 2011b). More information about the galaxy clusters in this table can be found in Mehrtens et al. (2011). Several of these clusters have more than one alternative name. For example, MaxBCG J229.07472+00.08903 is also known as Abell 2050 and RXC J1516.3+0005. Therefore, in order to be succinct, for each cluster in this table, we chose to present only the alternative name associated with the galaxy cluster that appears closest to the location of the XCS cluster when a query is submitted to NASA/IPAC Extragalactic Database (NED) (http://ned.ipac.caltech.edu/).

Cluster ID	Alternative name	z	L_{bol}^d	L_{bol}	T_X^d	T_X	Y	P_{full}
XMMXCS J151618.6+000531.3	MaxBCG J229.07472+00.08903	0.12	$4.4^{+0.1}_{-0.1}$	$4.4^{+0.1}_{-0.1}$	$5.4^{+0.1}_{-0.1}$	$5.3^{+0.1}_{-0.1}$	$0.3^{+0.1}_{-0.1}$	1.00/1.00
XMMXCS J104044.4+395710.4	ABELL 1068	0.14	$8.4^{+0.2}_{-0.2}$	$8.2^{+0.2}_{-0.2}$	$3.5^{+0.1}_{-0.1}$	$3.6^{+0.1}_{-0.1}$	$0.4^{+0.1}_{-0.1}$	1.00/1.00
XMMXCS J030348.3−775241.3*	1RXS J030344.4−775222	0.27	$16.2^{+0.4}_{-0.4}$	$16.3^{+0.3}_{-0.4}$	$8.7^{+0.3}_{-0.3}$	$8.3^{+0.3}_{-0.3}$	$1.0^{+0.2}_{-0.1}$	1.00/1.00
XMMXCS J122658.1+333250.9	WARP J1226.9+3332	0.89	$47.9^{+1.2}_{-1.1}$	$47.6^{+1.1}_{-1.1}$	$11.1^{+0.5}_{-0.5}$	$11.4^{+0.4}_{-0.4}$	$1.8^{+0.3}_{-0.2}$	1.00/1.00
XMMXCS J133254.8+503153.1*	RBS 1283	0.28	$12.5^{+0.4}_{-3.7}$	$12.7^{+0.3}_{-0.2}$	$7.7^{+0.3}_{-0.4}$	$7.3^{+0.4}_{-0.3}$	$0.8^{+0.1}_{-0.1}$	1.00/1.00
XMMXCS J111515.6+531949.5	SDSS J1115+5319 CLUSTER	0.47	$20.5^{+0.1}_{-0.1}$	$20.5^{+0.1}_{-0.1}$	$5.4^{+1.5}_{-0.9}$	$8.3^{+0.4}_{-0.4}$	$1.1^{+0.2}_{-0.2}$	0.99/1.00
XMMXCS J090101.5+600606.2	MaxBCG J135.25325+60.10133	0.29	$19.1^{+3.9}_{-3.2}$	$16.7^{+3.1}_{-2.8}$	$5.9^{+2.9}_{-1.4}$	$7.7^{+0.6}_{-0.6}$	$1.0^{+0.2}_{-0.2}$	1.00/1.00
XMMXCS J113020.3−143629.7*	ABELL 1285	0.11	$5.7^{+4.5}_{-1.7}$	$4.5^{+1.1}_{-1.0}$	$5.4^{+0.7}_{-0.7}$	$5.0^{+0.5}_{-0.4}$	$0.3^{+0.1}_{-0.1}$	1.00/1.00
XMMXCS J033049.7−522836.5	ABELL 3128 NE	0.44	$20.9^{+0.2}_{-0.2}$	$20.9^{+0.2}_{-0.1}$	$4.5^{+0.1}_{-0.1}$	$4.9^{+0.1}_{-0.1}$	$0.8^{+0.1}_{-0.1}$	0.71/1.00
XMMXCS J021440.9−043321.9	ABELL 0329	0.14	$2.8^{+3.4}_{-1.6}$	$3.1^{+0.6}_{-0.5}$	$4.5^{+0.1}_{-0.1}$	$4.5^{+0.1}_{-0.2}$	$0.2^{+0.1}_{-0.1}$	0.76/1.00
XMMXCS J004624.5+420429.5	RX J0046.4+4204	0.30	$7.0^{+0.3}_{-0.3}$	$7.0^{+0.3}_{-0.3}$	$6.9^{+0.6}_{-0.6}$	$6.0^{+0.3}_{-0.3}$	$0.5^{+0.1}_{-0.1}$	0.19/0.98
XMMXCS J141832.3+251104.9	WARP J1418.5+2511	0.29	$6.3^{+0.5}_{-0.5}$	$6.4^{+0.4}_{-0.5}$	$6.4^{+0.4}_{-0.4}$	$5.9^{+0.3}_{-0.3}$	$0.4^{+0.1}_{-0.1}$	0.13/0.94
XMMXCS J123019.6+161634.1	NSC J123020+161652	0.20	$4.6^{+0.8}_{-0.7}$	$4.0^{+0.7}_{-0.5}$	$4.3^{+0.6}_{-0.5}$	$4.7^{+0.4}_{-0.3}$	$0.3^{+0.1}_{-0.1}$	0.25/0.90
XMMXCS J121744.6+472921.5	400d J1217+4729	0.27	$23.2^{+13.2}_{-10.9}$	$8.4^{+6.1}_{-3.4}$	$9.8^{+6.6}_{-3.7}$	$6.1^{+1.3}_{-1.0}$	$0.5^{+0.4}_{-0.2}$	0.64/0.85
XMMXCS J095343.6+694735.0	400d J0953+6947	0.21	$1.0^{+3.0}_{-0.7}$	$3.6^{+1.7}_{-1.3}$	$5.7^{+1.1}_{-0.7}$	$4.7^{+0.6}_{-0.5}$	$0.3^{+0.1}_{-0.1}$	0.22/0.56

been evaluated outside this interval). Hereafter, these clusters will be referred to as constituting the XCS250 sample. In Table 1, all XCS250 clusters which have $P_{full}(>Y_{min}|L, T) > 0.5$ are presented. Note that even if this probability threshold was decreased to 0.01, only 7 (13 for the extended mission) more clusters would be added to Table 1.

Clearly, *Planck* will be able to detect only the closest, most luminous and hot clusters in the XCS. This can be also seen in Fig. 1, where we plot the minimum X-ray temperature, marginalized over X-ray luminosity and as a function of redshift, that an XCS cluster with over 250 X-ray photon counts needs to have in order to be
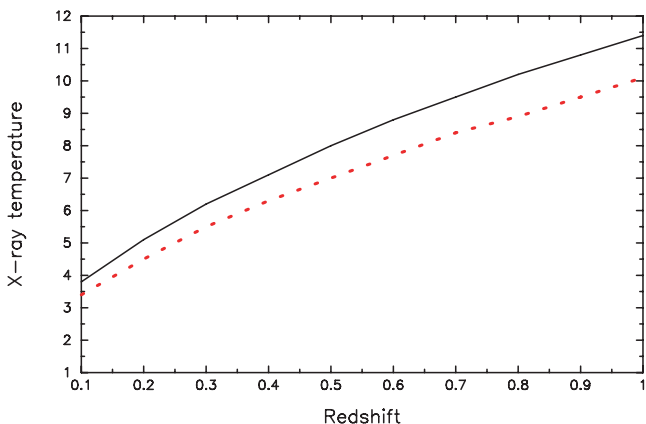

Figure 1. Minimum X-ray temperature, as a function of redshift, that an XCS cluster with over 250 X-ray photon counts needs to have in order to be detected by *Planck* with 0.5 probability (nominal mission – black/full, extended mission – red/dashed).

detected by *Planck* with 0.5 probability, for both the nominal and extended missions. Its substantial increase with redshift is a consequence of the characteristics of the *Planck* Cluster Survey selection function, given that the minimum cluster mass, and hence X-ray temperature and luminosity, above which *Planck* can detect galaxy clusters grows strongly with redshift (Melin et al. 2006; Planck Collaboration 2011b). It was therefore not a surprise to find that all the clusters in Table 1 had already been detected in previous surveys (Mehrtens et al. 2011). Interestingly, the clusters XMMXCS J030348.3−775241.3 (ie. PLCKESZ G294.66−37.02), XMMXCS J133254.8+503153.1 (i.e. PLCKESZ G107.11+65.31), XM-MXCS J113020.3−143629.7 (i.e. PLCKESZ G275.21+43.92), are already present in the *Planck* ESZ catalogue (Planck Collaboration 2011b), and have been found to have values for Y (Planck Collaboration 2011a), after rescaling to the same cluster radius, that are compatible within the uncertainties with those presented in Table 1. As expected, none of the XCS250 clusters not in Table 1 appear in the ESZ catalogue.

The methodology developed in the previous section can also be used to estimate the probability distributions for the bolometric luminosity, L_{bol}, X-ray temperature, T_X, and integrated Comptonization parameter, Y, associated with any XCS cluster. We have found that such distributions are close to log-normal, and calculated for each cluster in Table 1 the most probable values for L_{bol}, T_X and Y, as well as the respective 68 per cent confidence limits. In Table 1, the quantities L_{bol}^d and T_X^d are also shown. They differ from L_{bol} and T_X in that they were derived solely based on an analysis of the XCS data (Mehrtens et al. 2011). Given that the estimation of L_{bol} and T_X also depends on the (prior) assumptions regarding the cosmological model, cluster scaling relations and XCS selection function, the differences between the two sets of quantities gives an indication of

the tension between the cluster data and the theoretical framework considered, which we discuss next.

The assumed cosmological model predicts steeply decreasing cluster mass, temperature and luminosity functions, and thus this prior tends to make L_{bol} and T_X smaller than the equivalent data-based estimates. For example, this effect contributed to the significant reductions in the expected values for the bolometric luminosity and X-ray temperature of cluster XMMXCS J121744.6+472921.5, given that a cluster with a bolometric luminosity of 2.3×10^{45} erg s^{-1} and X-ray temperature of 9.8 keV would be so massive, and thus so rare, that it would be highly unlikely to be detected in the present cosmological volume probed by the XCS. However, how small L_{bol} and T_X can be, relative to their equivalent data-based estimates, will depend strongly on the magnitude of the uncertainties in the latter. For example, although the cluster XMMXCS J122658.1+333250.9 has higher L_{bol}^d and T_X^d than XMMXCS J121744.6+472921.5, the low uncertainty in its X-ray temperature data-based estimate does not allow the prior on the cosmological model forced to a prediction for the ratio T_X/T_X^d as low as in the case of XMMXCS J121744.6+472921.5.

The XCS selection function has an opposite, but much smaller, effect to that produced by the assumed cosmological model: given that the lower the bolometric luminosity of a cluster the more unlikely is its detection by the XCS, the effect of the XCS selection function is to predict L_{bol} to be (slightly) higher than L_{bol}^d. Note that the dependence of the XCS selection function on the cluster X-ray temperature is not monotonic (Sahlén et al. 2009), and thus it is not possible to predict beforehand if just taking into consideration the XCS selection function will result in a value for T_X that is higher or lower than T_X^d.

Finally, the cluster scaling relations, here assumed to be those derived from the pre-heating MGS, can also have a very strong effect on the estimates for L_{bol} and T_X, by forcing these quantities to comply with them. This may result in a higher T_X with respect to T_X^d, as happened to clusters XMMXCS J111515.6+531949.5 and XMMXCS J090101.5+600606.2, or in a lower T_X with respect to T_X^d, as was the result for the cluster XMMXCS J095343.6+694735.0. Essentially, the former have a value for L_{bol}^d that is significantly higher than the scaling relations predict given their T_X^d, while for the latter the situation is reversed.

Assuming that the final XCS catalogue will correspond to effectively searching a sky area of 600 deg^2 for serendipitous clusters, we have generated 20 000 random mock catalogues of the expected overlap between the XCS and *Planck* Cluster Survey, under the assumptions previously described. In Fig. 2, we plot the distribution thus obtained for the expected total number of galaxy clusters, with X-ray temperatures in excess of 2 keV and in the redshift interval $0.1 < z < 1.0$, as well as enough X-ray photon counts (>250) for their X-ray temperature to be estimated from the serendipitous X-ray data alone, that will be simultaneously detected by the XCS and *Planck* Cluster Survey. Unfortunately, the expected overlap has a most probable size of only 7 (3–13 with 95 per cent confidence) clusters for the nominal *Planck* mission, although it increases to 15 (8–23 with 95 per cent confidence) clusters for the extended *Planck* mission. However, this calculation is sensitive to the assumptions made regarding the fiducial cosmology, the normalization and covariance of the cluster scaling relations, and the characteristics of the XCS selection function and *Planck* sensitivity. For example, increasing/decreasing the assumed value for σ_8 by 5 per cent induces an increase/decrease of the expected number of overlapping clusters to 12/4 (23/9 for the extended mission). In Fig. 3, we plot the mean distribution of the properties of the galaxy clusters that appear
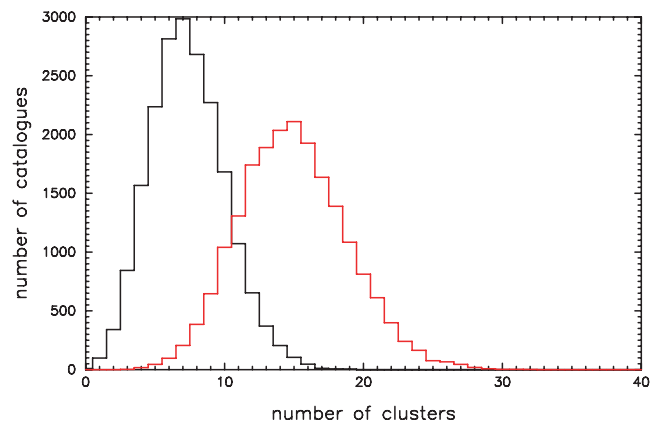

Figure 2. Probability distribution of the expected total number of galaxy clusters, with X-ray temperatures in excess of 2 keV and in the redshift interval $0.1 < z < 1.0$, that will be simultaneously detected by the XCS (with more than 250 X-ray photon counts) and *Planck* Cluster Survey over 600 deg^2 of sky (nominal mission – black, on the left, extended mission – red, on the right).

in the 20 000 random mock catalogues of the expected overlap between the XCS and *Planck* Cluster Survey, both for the nominal and extended missions, as well as the properties of the galaxy clusters presented in Table 1.

However, if we assume the XCS will keep finding clusters suitable for *Planck* detection at the same rate as up until now, then the number of clusters in Table 1, which correspond to an effective survey sky area of 410 deg^2, suggest the expected overlap between the final XCS catalogue and *Planck* Cluster Survey should be 16/22 clusters (nominal/extended cases). But such high numbers were only recovered in 68/1021 (nominal/extended cases) out of the 20 000 random mock catalogues that were generated of the expected overlap between the XCS and *Planck* Cluster Survey. The mismatch between the theoretical and the empirical estimates cannot be solved as easily as one could imagine, given the uncertainty associated with all the priors that influence the outcome of the theoretical predictions. This is because modifying most of those priors leads to changes in the theoretical and the empirical estimates that go in the same way. For example, assuming better sensitivity for *Planck* would lead to an increase in the theoretical expectation for the overlap between the XCS and *Planck* Cluster Survey as well as in the number of clusters in Table 1. The same would happen if the assumed normalizations of the scaling relations between cluster observables and cluster mass were increased. However, increasing the value assumed for σ_8, or assuming the XCS to be more sensitive, would lead to an increase in the theoretical expectation for the overlap between the XCS and *Planck* Cluster Survey without changing much the number of clusters in Table 1.

Alternatively, the X-ray luminosity of some of the galaxy clusters in Table 1 could have been increased by the presence of cool cores or mergers, whose effects may not have been properly modelled within the MGS, as well as due to active galactic nucleus contamination. This would lead to an overestimation of Y, and thus also of the probability of *Planck* detection, because Y is estimated from the pre-heating MGS scaling relations, given the observed value for the X-ray luminosity (as well as redshift and temperature) for each cluster.

Our simulations suggest that *Planck* will detect about 630 galaxy clusters, with X-ray temperatures in excess of 2 keV and in the redshift interval $0.1 < z < 1.0$, in the nominal mission, increasing
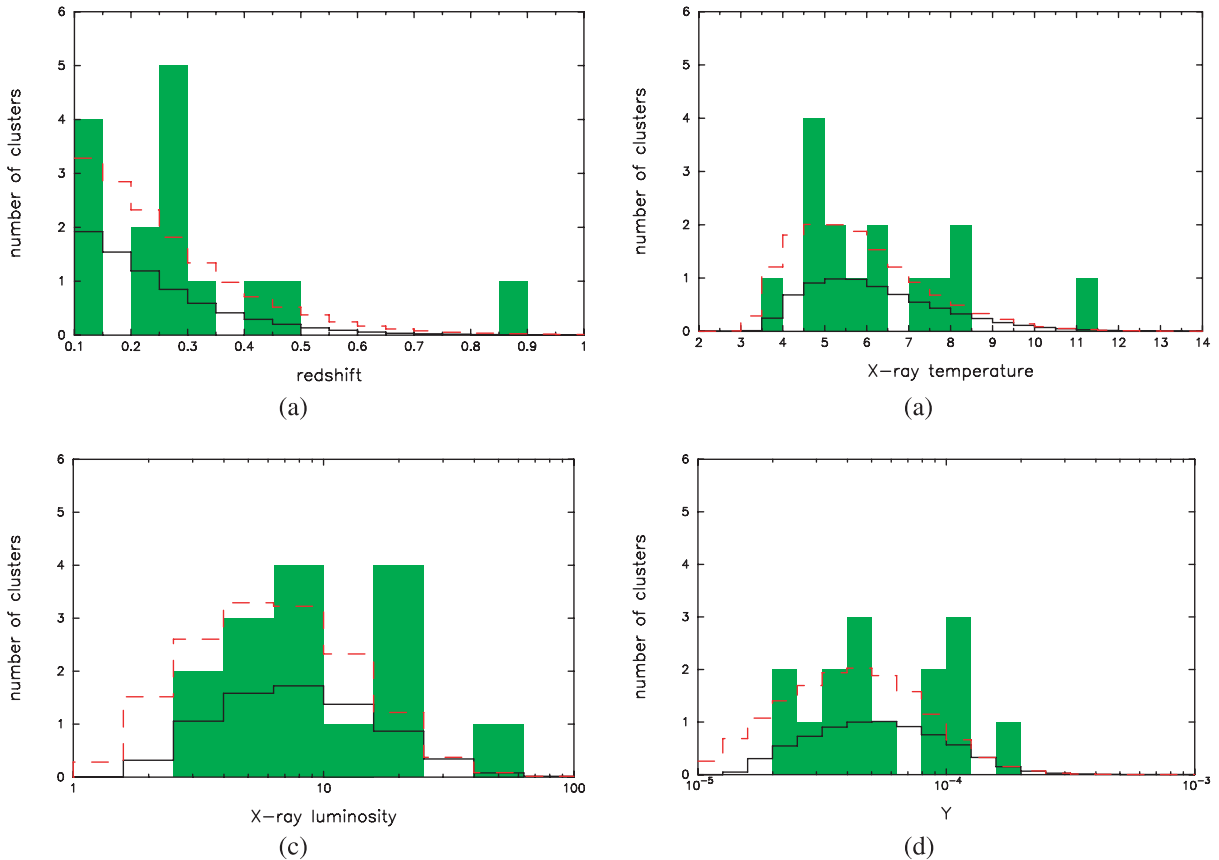
Figure 3. Mean distribution of the properties of the galaxy clusters that appear in the 20 000 randomly generated mock catalogues of the expected overlap between the XCS and *Planck* Cluster Survey (nominal mission – black/full, extended mission – red/long-dashed) and properties of the galaxy clusters presented in Table 1 (green, filled): (a) redshift; (b) X-ray temperature, T_X (in units of keV); (c) X-ray bolometric luminosity, L_{bol} (in units 10^{44} erg s^{-1}); (d) integrated Comptonization parameter, Y (in units h^{-2} Mpc^2). Both L_{bol} and Y are defined within r_{200}.

to approximately 1300 for the extended mission. This assumes the 41 253 deg^2 of sky coverage adopted by Melin et al. (2006). Although our result is lower than what others have obtained for the *Planck* nominal mission (Melin et al. 2006; Bartlett et al. 2008; Leach et al. 2008; Chamballu et al. 2010), due to the different tools and assumptions made, the result for the scaling with mission duration that we obtained should be robust.

The results so far presented suggest that the information contained in just the XCS and *Planck* data will not allow a comprehensive characterization of the cross-correlations between the most important cluster X-ray and SZ properties, as a function of redshift. This will only be achieved if more data is gathered, through extensive follow-up of both surveys: they complement each other in terms of area and depth, while suffering from different selection biases. The XCS is, on average, deeper than the *Planck* Cluster Survey, and thus the XCS will contain almost all clusters detected by *Planck* in the sky area that is common to both surveys. Our simulations suggest that, at $z \sim 0.1$, almost 90 per cent of the galaxy clusters, with X-ray temperatures in excess of 2 keV, expected to be detected by *Planck* (in both the nominal and extended missions) will also be detected by the XCS (with more than 50 photon counts), slowly decreasing to slightly more than 70 per cent at $z \sim 1$ (due to the existence of observations with low exposure times in the *XMM* archive). This means that the XCS will not only be able to help better characterize the sensitivity of the *Planck* Cluster Survey, which is essential in order to recover the scaling relations pertaining to the underlying galaxy cluster population, but will also enable *Planck* to

recover some information on many of the galaxy clusters that are just below its detection threshold in the sky area that is common to both surveys.

5 CONCLUSIONS

We have characterized the galaxy clusters, with X-ray temperatures in excess of 2 keV and in the redshift interval $0.1 < z < 1.0$, that are expected to be simultaneously detected by the XCS (with more than 250 X-ray photon counts) and *Planck* Cluster Survey. This overlap amounts to about 7/15 clusters for the nominal/extended *Planck* missions, taking the flat Lambda cold dark matter (ΛCDM) cosmology most compatible with *WMAP*7 data and with the covariance of the cluster X-ray luminosity, temperature, and integrated Comptonization parameter, as a function of cluster mass and redshift, determined by the pre-heating MGS. Under these assumptions, we have identified 11/15 clusters of galaxies in the first data release of the XCS catalogue, with a minimum of 250 X-ray photon counts, X-ray temperatures in excess of 2 keV and in the redshift interval $0.1 < z < 1.0$, that have more than a 50 per cent chance of being detected by *Planck* at the end of its nominal/extended missions. Both results clearly show that *Planck* will be able to detect only the closest, most luminous and hot clusters in the XCS.

The galaxy clusters that appear in both the XCS and *Planck* Cluster Survey will provide valuable insights into the cross-correlations of X-ray and SZ properties, but their small number will not allow for the comprehensive characterization of such correlations.

However, being on average the deeper of the two surveys, the XCS will help determine better the selection function of the *Planck* Cluster Survey. In the sky area that is common to both surveys, the XCS will also make possible the recovery of some information on many of the galaxy clusters that are just below the *Planck* detection threshold (Planck Collaboration 2011c), as well as significantly improve the *Y* estimates for all clusters detected by *Planck* by aiding in the determination of cluster size (Planck Collaboration 2011b).

REFERENCES

Annis J. et al., 2005, White Paper submitted to the Dark Energy Task Force, preprint (arXiv:astro-ph/0510195)
Bartlett J. G., Chamballu A., Melin J.-B., Arnaud M., Members of the Planck Working Group 5, 2008, Astron. Nachr., 329, 147
Böhringer H. et al., 2000, ApJS, 129, 435
Böhringer H. et al., 2004, A&A, 425, 367
Burenin R. A., Vikhlinin A., Hornstrup A., Ebeling H., Quintana H., Mescheryakov A., 2007, ApJS, 172, 561
Cappelluti N. et al., 2011, Mem. Soc. Astron. Ital., 17, 159
Carlstrom J. E., Holder G. P., Reese E. D., 2002, ARA&A, 40, 643
Carlstrom J. E. et al., 2011, PASP, 123, 568
Chamballu A., Bartlett J. G., Melin J. -B., 2010, A&A, preprint (arXiv:1007.3193)
Cruddace R. et al., 2002, ApJS, 140, 239
De Grandi S. et al., 1999, ApJ, 514, 148
Ebeling H., Edge A. C., Böhringer H., Allen S. W., Crawford C. S., Fabian A. C., Voges W., Huchra J. P., 1998, MNRAS, 301, 881
Henry J. P., Gioia I. M., Mullis C. R., Voges W., Briel U. G., Böhringer H., Huchra J. P., 2001, ApJ, 553, L109
Hu W., Kravtsov A. V., 2003, ApJ, 584, 702
Jenkins A., Frenk C. S., White S. D. M., Colberg J. M., Cole S., Evrard A. E., Couchman H. M. P., Yoshida N., 2001, MNRAS, 321, 372
Kay S. T., da Silva A. C., Aghanim N., Blanchard A., Liddle A. R., Puget J.-L., Sadat R., Thomas P. A., 2007, MNRAS, 377, 317
Komatsu E. et al., 2010, ApJS, 192, 18
Leach S. M. et al., 2008, A&A, 491, 597
Lloyd-Davies E. J. et al., 2011, MNRAS, 418, 14
Marriage T. A. et al., 2010, ApJ, 737, 61
Mehrtens N. et al., 2011, MNRAS, preprint (arXiv:1106.3056)
Melin J.-B., Bartlett J. G., Delabrouille J., 2006, A&A, 459, 341
Mullis C. R. et al., 2003, ApJ, 594, 154
Perlman E. S., Horner D. J., Jones L. R, Scharf C. A., Ebeling H., Wegner G., Malkan M., 2002, ApJS, 140, 265
Planck Collaboration, 2011a, A&A, 536, A1
Planck Collaboration, 2011b, A&A, 536, A8
Planck Collaboration, 2011c, A&A, 536, A10
Romer A. K. et al., 2000, ApJS, 126, 209
Romer A. K., Viana P. T. P., Liddle A. R., Mann R. G., 2001, ApJ, 547, 594
Rosati P., Della Ceca R., Burg R., Norman C., Giacconi R., 1998, ApJ, 492, L21
Sahlén M. et al., 2009, MNRAS, 397, 577
Stanek R., Rasia E., Evrard A. E., Pearce F., Gazzola L., 2010, ApJ, 715, 1508
Vanderlinde K. et al., 2010, ApJ, 722, 1180
Williamson R. et al., 2011, ApJ, 738, 139

This paper has been typeset from a TeX/LaTeX file prepared by the author.